Stress partition and microstructure in size-segregating granular flows

L. Staron[1,2,3,*] and J. C. Phillips[3]

[1]*Sorbonne Université, UPMC Université Paris 06, UMR 7190, Institut Jean Le Rond d'Alembert, F-75005 Paris, France*

[2]*CNRS, UMR 7190, Institut Jean Le Rond d'Alembert, F-75005 Paris, France*

[3]*School of Earth Sciences, University of Bristol, Bristol BS8 1TH, United Kingdom*

(Received 21 January 2015; revised manuscript received 29 April 2015; published 25 August 2015)

When a granular mixture involving grains of different sizes is shaken, sheared, mixed, or left to flow, grains tend to separate by sizes in a process known as size segregation. In this study, we explore the size segregation mechanism in granular chute flows in terms of the pressure distribution and granular microstructure. Therefore, two-dimensional discrete numerical simulations of bidisperse granular chute flows are systematically analyzed. Based on the theoretical models of J. M. N. T. Gray and A. R. Thornton [Proc. R. Soc. A **461**, 1447 (2005)] and K. M. Hill and D. S. Tan [J. Fluid Mech. **756**, 54 (2014)], we explore the stress partition in the phases of small and large grains, discriminating between contact stresses and kinetic stresses. Our results support both gravity-induced and shear-gradient-induced segregation mechanisms. However, we show that the contact stress partition is extremely sensitive to the definition of the partial stress tensors and, more specifically, to the way mixed contacts (i.e., involving a small grain and a large grain) are handled, making conclusions on gravity-induced segregation uncertain. By contrast, the computation of the partial kinetic stress tensors is robust. The kinetic pressure partition exhibits a deviation from continuum mixture theory of a significantly higher amplitude than the contact pressure and displays a clear dependence on the flow dynamics. Finally, using a simple approximation for the contact partial stress tensors, we investigate how the contact stress partition relates to the flow microstructure and suggest that the latter may provide an interesting proxy for studying gravity-induced segregation.

DOI: 10.1103/PhysRevE.92.022210 PACS number(s): 45.70.−n, 05.65.+b

I. INTRODUCTION

When a granular mixture involving grains of different sizes is shaken, sheared, mixed, or left to flow, grains tend to separate by sizes in a process known as size segregation. In the simple case of free surface flow under gravity, larger grains rise to the surface while smaller grains sink at the bottom of the flow. Segregation occurs in a wide variety of contexts—either industrial or natural [1–6]—for which it represents an engineering and scientific challenge. Kinetic theory offers a well-established framework to describe segregation in dilute granular systems [7,8]; however, its applicability is limited in the case of dense flows, where grains interact through long-lasting contacts rather than binary collisions. Since the seminal work by Savage and Lun [9] and the introduction of the *random kinetic sieve*, much progress has been achieved in understanding segregation mechanisms, both experimentally [10–22] and using numerical simulations [23–32]. In this respect, because they allow for very well-controlled configurations and provide access to the inner structure of the flow, discrete numerical simulations have proven a fruitful tool and provide significant insight to inform continuum modeling [4,30,33–36].

One of the challenges posed by granular size segregation lies in the task of identifying the actual driving mechanisms [27,31,33,37–39]. Experimental evidence for the lift force that drives an intruder upwards in a quasistatic shear flow was recently given and shown to scale like Archimedes force [16]. It seems reasonable to suppose that such lift forces are at play in size-disperse dense granular flows, although the dependences on the flow composition and dynamics have to be established. In the absence of an explicit generic formulation for the segregation force, a fruitful hypothesis was proposed by Gray and Thornton [33]: smaller grains, while percolating through the network of larger grains, are screened from average stress and thus carry less of the lithostatic pressure than larger grains do. This hypothetical mechanism translates mathematically into a departure from classical continuum mixture theory; it allows for the recovery of important features of segregation in depth-averaged equations [33]. It has since been the subject of various improvements [29,30,34,38]. Yet the basic ingredient, namely, the fact that the partial pressure in the phase of smaller grains is less than simply proportional to their volume occupation, has to be unambiguously established. While Weinhart *et al.* do observe such asymmetry in discrete numerical simulations [39], the results obtained by Fan and Hill [27] and Hill and Tan [31] are inconsistent with this hypothesis. More recently, it was proposed by Fan and Hill that, in addition to gravity—or in place of it—kinetic stresses play a crucial role in size segregation [37]. They identify the gradients of velocity fluctuations as the driving mechanism [27,31].

Based on the theoretical models of Gray and Thornton [33] and Hill and Tan [31], we explore the stress partition in the phases of small and large grains, discriminating between contact stress and kinetic stress, in numerical bidisperse granular flows. The numerical method and simulation are presented in Sec. II. Contact stresses and their partition between small- and large-grain phases are analyzed in Sec. III. Section IV explores the partition of kinetic stresses and its sensitivity to the flow dynamics. The relation between contact stresses and granular microstructure is established in Sec. V. We finally discuss the results in Sec. VI.

*lydie.staron@upmc.fr

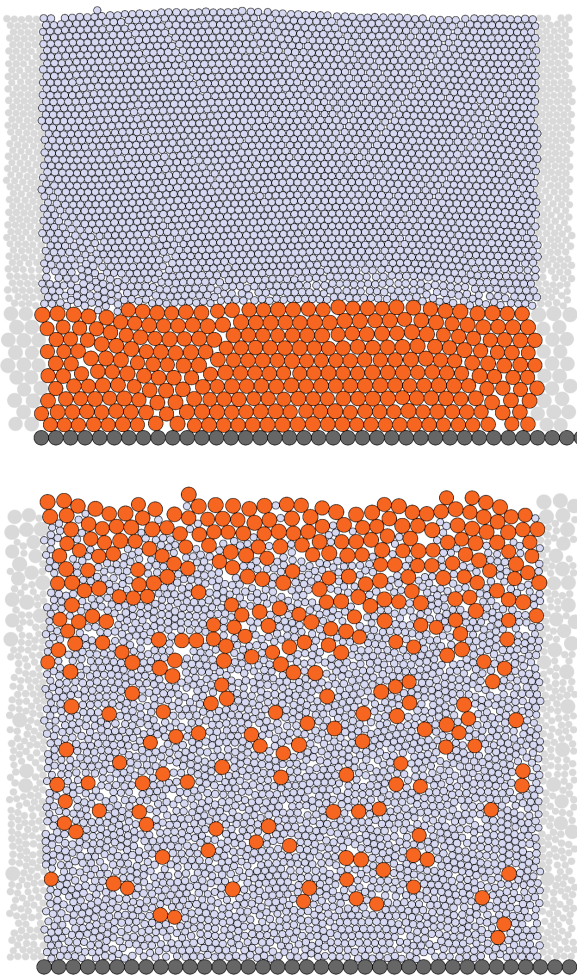

FIG. 1. (Color online) Example of bidisperse granular flow with the volume fraction of large beads $\Phi_L = 0.3$ in the initial state ($t = 0$) and after steady state is reached and segregation has occurred ($t = 150s$); the slope is $\theta = 23^\circ$. The ratio of the diameter of large grains to that ofsmall grains is $d_L/d_S = 2$ ($d_S = 0.005$ m).

II. NUMERICAL FLOWS

The numerical systems consist of two-dimensional (2D) granular beds of grains of two sizes allowed to flow under gravity on a fixed plane of slope θ made of grains of the larger size. As the flow develops, segregation occurs, and the larger grains—initially placed at the bottom of the granular layer—rise in the flow, as illustrated in Fig. 1. This typical chute flow experiment is, in principle, similar to those reported in [25,29,30,32].

This numerical experiment was performed using the contact dynamics algorithm [40,41], assuming perfectly rigid grains. The grains interact at contacts through solid friction: locally, the normal and tangential contact forces satisfy $f_t \leqslant \mu f_n$, where μ is the coefficient of friction at contact. Moreover, a coefficient of energy restitution e sets the amount of energy dissipated by collisions. The numerical values of μ and e control the effective frictional properties of the flow in a given configuration. They are strictly the same for all contacts between large and small grains. In this work, we are not interested in understanding how they may affect the segregation process, hence, their value is set to $\mu = 0.5$ and $e = 0.25$ and is not varied.

We denote d_L and d_S the mean diameter of large and small grains, respectively. To prevent geometrical ordering, likely to occur for strictly monosized packings, both large and small grains have diameters uniformly distributed around their mean value so that $\frac{(d_L^{\max}-d_L^{\min})}{d_L} = \frac{(d_S^{\max}-d_S^{\min})}{d_S} = 0.08$ (a discussion of the influence of this value on the segregation process is given in [32]). The ratio d_L/d_S was not varied: $d_L/d_S = 2$.

Periodic boundary conditions were implemented to ensure long flow durations; the width of the simulation cell is $35d_L$. The basal boundary is made of a row of fixed beads of diameter d_L. In the initial state, a layer of large beads is overlaid by a layer of small beads (Fig. 1). This is achieved by random deposition under gravity. We denote Φ^L the volume fraction of large beads at the flow scale, i.e., the ratio of the volume of large beads to the total volume of grains: $\Phi^L = V_L/(V_S + V_L)$. The volume fraction of small beads is $\Phi^S = (1 - \Phi^L)$. In the simulations, Φ^L is varied between 0.06 and 0.90. In addition, we define the local volume fraction of large and small beads ϕ^L and ϕ^S. The height of the granular bed in the initial state is H_0; irrespective of Φ^L, H_0 was kept constant and equal to $H \simeq 60d_S$. The slope of the granular bed θ was varied between 21° and 26°, allowing different flow velocities. The numerical values used for the simulations are the following: $d_S = 5 \times 10^{-3}$ m, $\rho = 1$ kg m^{-2}, and $g = 9.8$ m s^{-2}.

III. CONTACT STRESSES AND GRAVITY-DRIVEN SEGREGATION

Contact stresses are transmitted at contacts between grains during either short collisions or enduring contacts; its micromechanical expression is [42]

$$\boldsymbol{\sigma} = \frac{1}{V} \sum_{\alpha \in N_c} \vec{f}^{\alpha} \otimes \vec{\ell}^{\alpha}, \tag{1}$$

where $\vec{f}^{\alpha}$ is the force transmitted at the contact α, $\vec{\ell}^{\alpha}$ is the vector joining the centers of mass of the two grains involved, N_c is the number of contacts over which the summation is made, V is the volume over which the stress is computed, and $\otimes$ is the dyadic product. The eigenvalues λ_1 and λ_2 of this stress tensor give the pressure P: $P = (\lambda_1 + \lambda_2)/2$. A typical pressure profile is shown in Fig. 2(a) for a granular flow with $\Phi^L = 0.30$ flowing at an angle of 23° in the steady (i.e., segregated) state, as shown in Fig. 1. It simply obeys a lithostatic profile $P(z) = \rho g \cos\theta (H_0 - z)$, where z is the depth (counted from the bottom).

In bidisperse granular flows, contacts may involve only large grains, only small grains, or one large grain and one small grain. In the latter mixed case, a meaningful partition of the stress for computation of the partial stress tensors $\boldsymbol{\sigma}^S$ and $\boldsymbol{\sigma}^L$ is necessary. Following [39] and [31], the contribution of the mixed cases is distributed according to the size of the grains, namely, weighted by a prefactor $d_L/(d_L + d_S)$ or $d_S/(d_L + d_S)$ for the phase of large and small grains, respectively (we see that using a different partition changes the results dramatically). We thus define the partial stress tensors $\boldsymbol{\sigma}^L$ and $\boldsymbol{\sigma}^S$ and the corresponding partial pressures P^L and P^S. In the following,

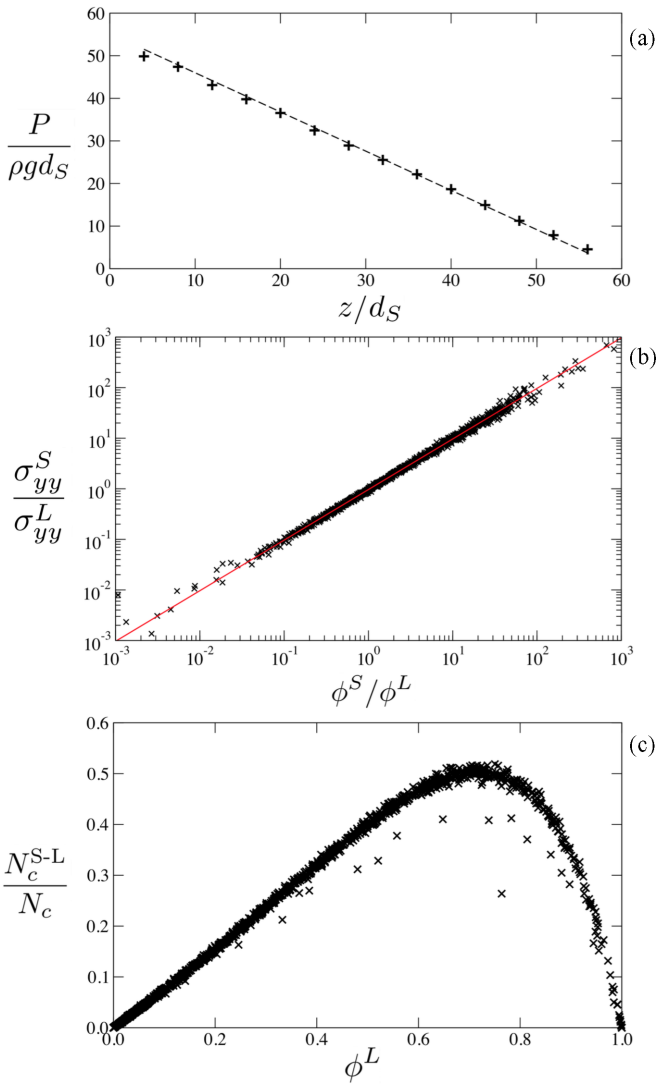

FIG. 2. (Color online) (a) Example of the pressure profile in a segregated flow with $\Phi^L = 0.3$ and $\theta = 23^\circ$; the dotted line shows $P = \rho g(H_0 - z)$. (b) Ratio of the partial contact stresses $\sigma^S_{yy}/\sigma^L_{yy}$ as a function of the local ratio of the volume fractions ϕ^S/ϕ^L for flows with $\Phi^L = 0.06$, 0.15, 0.30, 0.45, 0.60, and 0.75 and slope $\theta = 23^\circ$; the (red) line shows $\sigma^S_{yy}/\sigma^L_{yy} = 0.9660\,(\phi^S/\phi^L)$. (c) Proportion of mixed contacts (between one small and one large grain) as a function of the local volume fraction of large grains for $\Phi^L = 0.06$, 0.15, 0.30, 0.45, 0.60, and 0.75 and slope $\theta = 23^\circ$.

however, to allow precise comparison with earlier works, we mostly use the normal stress components σ^L_{yy} and σ^S_{yy}.

In the framework of classical continuum mixture theory, partial stresses are expected to be proportional to the mean stress σ_{yy} and to the volume fraction of the considered grain species in the mixture, namely, locally in the flow: $\sigma^L_{yy} = \phi^L\sigma_{yy}$ and $\sigma^S_{yy} = \phi^S\sigma_{yy}$. A departure from mixture theory as proposed in [33] implies, however, different stress partition coefficients $\psi^L \neq \phi^L$ and $\psi^S \neq \phi^S$ [27,39] such that $\psi^L + \psi^S = 1$ and

$$\sigma^L_{yy} = \psi^L\sigma_{yy},$$
$$\sigma^S_{yy} = \psi^S\sigma_{yy}.$$

Considering bidisperse flows with a volume fraction of large grains $\Phi^L = 0.06, 0.15, 0.30, 0.45, 0.60$, and 0.75, and flowing at an angle $\theta = 23^\circ$, we evaluate the local contact stresses σ^L_{yy} and σ^S_{yy} using Eq. (1), computed over horizontal layers of width $4d_S$ and over time intervals of 1.25 s. For the same volumes and time intervals, the local volume fractions of large and small grains ϕ^L and ϕ^S are also evaluated. We do not try to separate the early stages of the segregation from the later stages, as we found that it had no visible influence on the results reported hereafter. We can thus plot the stress ratio $\sigma^S_{yy}/\sigma^L_{yy}$ as a function of the volume fraction ratio ϕ^S/ϕ^L [Fig. 2(b)]. In order to filter out the extreme cases, the best fit is calculated for $0.01 < \phi^S/\phi^L < 100$. We find

$$\frac{\sigma^S_{yy}}{\sigma^L_{yy}} \simeq (0.9660 \pm 0.003)\frac{\phi^S}{\phi^L}, \tag{2}$$

which suggests a small asymmetry of the stress partition compared to a classical mixture. In the original model proposed by Gray and Thornton [33], the stress partition obeys the following law:

$$\psi^L = \phi^L(1 + B\phi^S), \tag{3}$$
$$\psi^S = \phi^S(1 - B\phi^L). \tag{4}$$

Using (2), (3), and (4) gives $B \simeq (1 - 0.9660)/(\phi^L + 0.9660(1 - \phi^L))$, namely, $0.034 < B < 0.035$. This value is larger than the value observed for 3D chute flows by Weinhart *et al.* (who find $B \simeq 0.02$) [39] and supports the plausibility of gravity-driven segregation in the system (note that Hill and Tan find $B \simeq 0$ for 3D rotating drums [31]).

It should be noted that the value of B is very sensitive to the details of the stress computation. For instance, considering the ratio of the partial pressures P^S/P^L rather than the ratio of the partial normal stresses $\sigma^S_{yy}/\sigma^L_{yy}$ gives $0.045 < B < 0.047$, namely, a larger value of B. Far more dramatic is the influence of the stress distribution at mixed contacts (between a large grain and a small grain) between the two phases. In the analysis above, the distribution of the stress transmitted at mixed contacts is weighted by the grain size, namely, a prefactor of 1/3 for the contribution to the phase of small grains and a prefactor of 2/3 for the contribution to the phase of large grains (since $d_L = 2d_S$). Changing the prefactors to 0.2 for the phase of small grains and 0.8 for the phase of large grains leads to $B \simeq 0.33$, namely, a massive increase. On the contrary, changing the prefactors to 0.4 and 0.6 leads to $B \simeq -0.1$, which is an inverse segregation process. Finally, changing the prefactors to 0.5 and 0.5 leads to $B \simeq -0.32$ and brings an entirely different picture. The strong influence of the way mixed contacts are taken into account in the stress computation can be explained by their proportion in the mixture, which can reach 50% locally, depending on the volume fraction of large grains, as shown in Fig. 2(c). This makes the interpretation of contact stress ratios awkward, particularly if one wants to compare mixtures with different grain sizes. In that case, the ponderation using grain sizes to split contact forces in the partial stress computation effectively introduces a dependence on the grain size. This dependence may affect the relative values of partial stresses, and introduce a bias in the interpretation of the results. In other words,

understanding the role of grains sizes in stress partition becomes uneasy if grains sizes are used at first to define partial stresses.

No influence of the slope angle θ (that is, of the flow velocity) on the value of B was observed.

IV. KINETIC STRESSES AND SHEAR-GRADIENT-INDUCED SEGREGATION

Kinetic stresses are related to the existence of velocity fluctuations in granular flows and can be quantified through an analog of the Reynolds stress tensor,

$$\boldsymbol{\sigma}^{\kappa} = \frac{1}{V}\sum_{i\in N_p} m_i \delta\vec{v}_i \otimes \delta\vec{v}_i, \tag{5}$$

where $\delta\vec{v}_i$ is the fluctuating velocity of the grain i, m_i its mass, and N_p the total number of grains in the volume V over which the stress is computed. A typical kinetic pressure profile is shown in Fig. 3(a) for a steady-state granular flow with $\Phi^L = 0.30$ flowing at an angle of 23°. The normalization by $\rho g d_S$ allows for quantitative comparison with the contact stress profile shown in Fig. 2. Kinetic stresses are about four orders of magnitude smaller than contact stresses, namely, seemingly negligible. However, as stressed in [31] and [37], the difference in behavior between the phase of small grains and the phase of large grains is more striking than for contact stresses. Computing the partial kinetic stress tensors $\boldsymbol{\sigma}^{\kappa,S}$ and

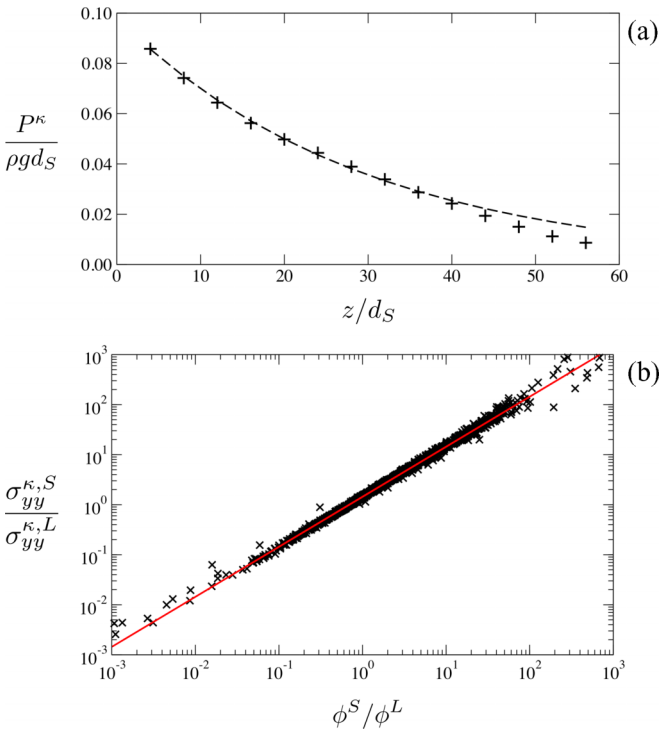

FIG. 3. (Color online) (a) Profile of the kinetic pressure P^κ (normalized by $\rho g d_S$) for a granular flow with $\Phi^L = 0.30$ and $\theta = 23°$ at steady state; the dotted line shows the best fit $P^\kappa = 0.98e^{-z/(14.8d_L)}$. (b) Ratio of the local partial kinetic stresses $\sigma^{\kappa,S}_{yy}/\sigma^{\kappa,L}_{yy}$ as a function of the ratio of the local volume fractions ϕ^S/ϕ^L for $\Phi^L = 0.06$, 0.15, 0.30, 0.45, 0.60, and 0.75 and slope $\theta = 23°$; the solid (red) line shows the best fit $y = 1.44x^{1.0057}$

$\boldsymbol{\sigma}^{\kappa,L}$ is straightforward, as it implies a summation on the grains and not on the contacts. Plotting the kinetic stress ratio $\sigma^{\kappa,S}_{yy}/\sigma^{\kappa,L}_{yy}$ as a function of the volume fraction ratio ϕ^S/ϕ^L [Fig. 3(b)], we find

$$\frac{\sigma^{\kappa,S}_{yy}}{\sigma^{\kappa,L}_{yy}} \simeq (1.4413 \pm 0.0022)\left(\frac{\phi^S}{\phi^L}\right)^{1.0057}.$$

The prefactor 1.4413 implies that smaller grains experience more of the kinetic stress than larger grains, i.e., they undergo larger velocity fluctuations. Since they are geometrically less constrained than larger grains due to their size, this result is expected. Interpreting this value in the framework of the model of Gray and Thornton [33], namely, introducing a kinetic pressure partition coefficient B_κ such that

$$\sigma^{\kappa,L}_{yy} = \phi^L(1 + B_\kappa\phi^S)\sigma^{\kappa}_{yy}, \tag{6}$$

$$\sigma^{\kappa,S}_{yy} = \phi^S(1 - B_\kappa\phi^L)\sigma^{\kappa}_{yy}, \tag{7}$$

gives a large negative pressure partition coefficient $B_\kappa \simeq -0.373$, similar to the values observed in [31] and [39] for 3D flows ($B_\kappa \simeq -0.39$ and $B_\kappa \simeq -0.38$, respectively). The value of B_κ is more then 10 times larger than the pressure partition coefficient measured for contact stresses in Sec. III and supports the proposition of a segregation mechanism driven by granular temperature by [31]. In the chute flow configuration, large grains are segregated towards the cooler regions of the flow (namely, the surface) as predicted by kinetic theory [43] but differently from what is observed in rotating drums, for which the flow surface coincides with a higher granular temperature [31].

We can show that the value of B_κ is sensitive to the mean shear rate. Simulating granular flows with $\Phi^L = 0.45$, and with varying slopes $\theta = 21°$, 22°, 23°, 24°, 25°, and 26°, we compute the ratio $\sigma^{\kappa,S}_{yy}/\sigma^{\kappa,L}_{yy}$ for each case and fit the dependence on ϕ^S/ϕ^L with a linear law. We then derive the mean value of B_κ from relations (6) and (7). The plot of B_κ as a function of the normalized shear rate is displayed in Fig. 4; we observe a monotonous increase with $\dot{\gamma}/\sqrt{g/d_S}$. From the analysis of the segregation time scales for similar 2D numerical flows [32], this increase in B_κ corresponds to a shorter segregation time, i.e., a higher segregation velocity. However, it does not coincide with a higher segregation rate, as the final position of the center of gravity of the large grains was shown to remain unaffected by an increasing mean shear rate [32].

V. MICROSTRUCTURAL SIGNATURE

While one can easily picture why smaller grains are submitted to larger kinetic stresses (simply as a result of their greater degrees of freedom), the fact that they sustain a smaller proportion of the contact stresses than their volume proportion is less intuitive. From the micromechanical definition of the contact stress tensor given in (1), we can try to approximate the partial pressures by the mean forces and the mean coordinance number in each phase of grains.

If N_c^L is the number of contacts involving at least one large grain, f_L the mean modulus of the forces transmitted by these contacts (in which a least one large grain is involved), and

ℓ_L the mean distance between the centers of mass of the two grains in contacts, then an estimate Π^L of the partial pressure P^L supported by the large grains is [following (1)]

$$\Pi^L \simeq \frac{1}{V} N_c^L f_L \ell_L.$$

The number of contacts N_c^L involving at least one large grain can be estimated from the number of large grains n_L, and their coordination number z_L (i.e., the number of contacts that a large grain experiences on average): $N_L = n_L z_L/2$. The volume occupied by large grains is $\phi^L V$; the mean diameter of the large grains being d_L, we estimate their number $n_L = \phi^L V/(\pi d_L^2/4)$. Finally, ℓ_L can be approximated by the diameter of one large grain, $\ell_L \simeq d_L$. This gives the following estimate for the magnitude of the partial pressure supported by large grains:

$$\Pi^L \simeq \frac{2}{\pi d_L} z_L f_L \times \phi^L. \tag{8}$$

In the same way, N_c^S being the number of contacts involving at least one small grain, f_S the mean modulus of the forces transmitted by these contacts (in which a least one small grain is involved), and ℓ_S the mean distance between the centers of mass of the two grains in contact, an estimate Π^S of the partial pressure P^S supported by small grains is

$$\Pi^S \simeq \frac{1}{V} N_S f_S \ell_S.$$

As before, $N_S = n_S \times z_S/2$. Smaller grains occupying a volume ϕ^S, their number is $n_S = \phi^S V/(\pi d_S^2/4)$. Finally, reasoning as for large grains, we suppose that $\ell_S \simeq d_S$ and eventually

$$\Pi^S \simeq \frac{2}{\pi d_S} z_S f_S \times \phi^S. \tag{9}$$

Both estimates, Π^S and Π^L, are derived from crude simplifications and are expected to provide only a rough guess of the real value of the partial pressures as calculated from (1). To quantify the error made when using (8) and

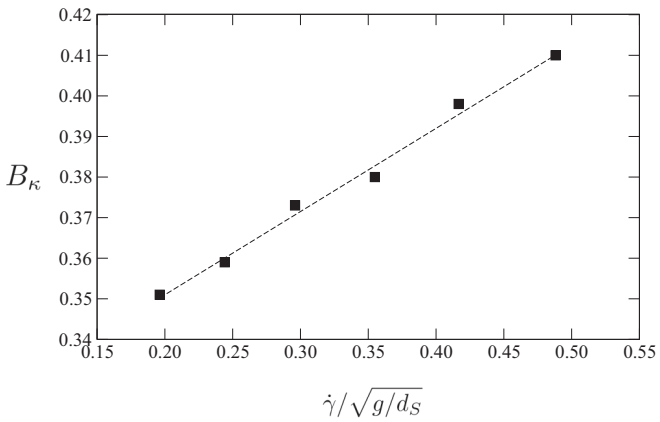

FIG. 4. Kinetic pressure partition coefficient B_κ as a function of the flow-normalized mean shear rate $\dot{\gamma}/\sqrt{g/d_S}$ computed for flows with a mean volume fraction of large grains $\Phi^L = 0.45$ and for slope angles varying from $\theta = 21^\circ$ to $\theta = 26^\circ$. The dotted line shows the best-fit trend $y = 0.310 + 0.205x$.

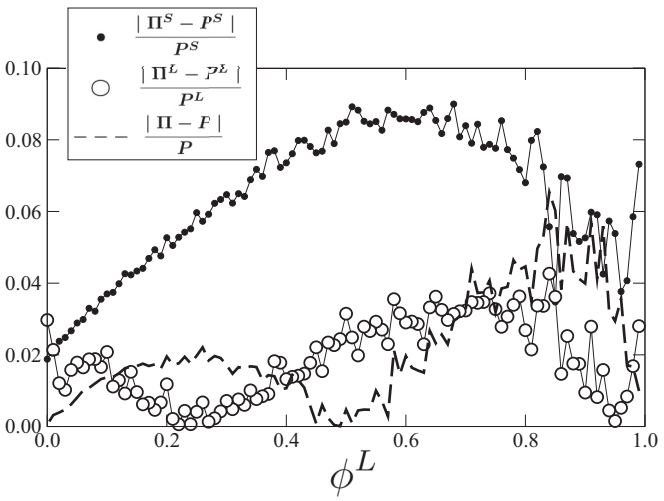

FIG. 5. Mean error of the approximations Π, Π^L, and Π^S of the pressures P, P^L, and P^S as a function of the volume fraction of large grains ϕ^L: for six flows with differing volume fractions of large grains, $\Phi^L = 0.06$, 0.15, 0.30, 0.45, 0.60, and 0.75, flowing at $\theta = 23^\circ$.

(9), we compare the values they provide for P^L and P^S with the exact computation presented in Sec. III, averaging over six flows with different volume fractions of large grains, $\Phi^L = 0.06$, 0.15, 0.30, 0.45, 0.60, and 0.75, and flowing at an angle $\theta = 23^\circ$. The results are shown in Fig. 5, where $|\Pi^S - P^S|/P^S$, $|\Pi^L - P^L|/P^L$, and $|\Pi - P|/P$ are reported as a function of ϕ_L. We see that in spite of the simplification, Π and Π^L give reasonable estimates of the value of P and P^L, with a maximum error of 3% and 5% and a mean error of 2.2% and 1.9%, respectively. The error on P^S is larger but remains less than 9% and has a mean value of 6.4%. We observe that the error is larger for a large proportion of mixed contacts between large and small grains, which is shown in Fig. 2(c). As noted before, mixed contacts are the main source of uncertainty when computing partial contact stresses.

If the approximations are too simple to give a quantitative estimate of the stress partition coefficient B, they are sufficient to give a qualitative picture of how B behaves with the flow microstructure. Returning to the model of Gray and Thornton [33], we write

$$\Pi^L = \phi^L(1 + B\phi^S)\,\Pi, \tag{10}$$

$$\Pi^S = \phi^S(1 - B\phi^L)\,\Pi, \tag{11}$$

as we did for σ_{yy}^L and σ_{yy}^S in Sec. III [Eqs. (3) and (4)]. Substituting Π^L and Π^S by their expressions (8) and (9) gives, for B,

$$B \simeq \frac{1 - r_d \frac{z_S f_S}{z_L f_L}}{\phi^L + r_d \frac{z_S f_S}{z_L f_L} \times \phi^S}, \tag{12}$$

where $r_d = d_L/d_S = 2$. From this analysis, we see that the main ingredient that controls the contact stress partition is the ratio of the mean force on small grains to the mean force on large grains: the lower this ratio, the more efficient the segregation. For $r_d = 2$, the condition for segregation (namely, $B > 0$) is that $z_S f^S < \frac{1}{2} z_L f^L$. We note also that the size ratio

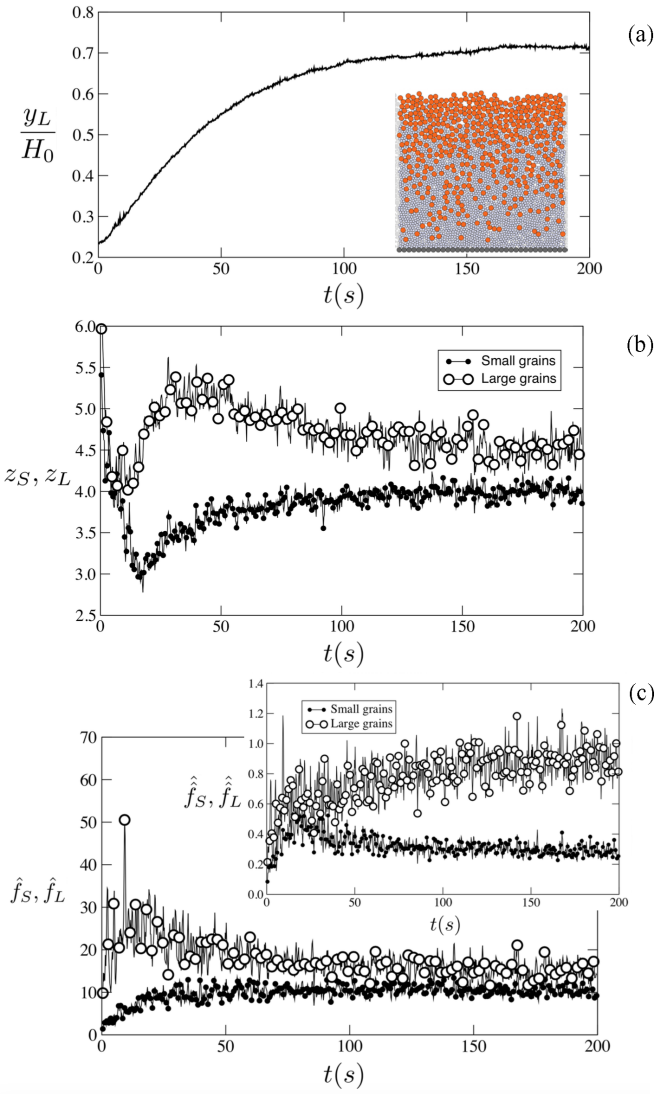

FIG. 6. (Color online) For a given flow with $\Phi^L = 0.45$ and $\theta = 23^\circ$: (a) vertical position of the center of mass of the large grains y_L normalized by the flow height H_0 over the course of time; (b) coordinance number for z_S and z_L for small (filled circles) and large (open circles) grains over the course of time; and (c) mean force transmitted by contact involving at least one small grain (filled circles) and one large grain (open circles) normalized by the weight of one small grain $m_S g$ ($\hat{f}_S$ and $\hat{f}_L$, respectively) and normalized by the pressure seen by their center of mass ($\hat{\hat{f}}_S$ and $\hat{\hat{f}}_L$, respectively; inset) as a function of time.

r_d is not explicitly favorable to stress partition but tends to decrease the value of B.

This microstructural condition for segregation can be observed from direct measurements of the mean force transmitted at contacts and direct measurement of the mean number of contacts in which grains are involved on average for each species. Considering a single flow ($\Phi^L = 0.45$, $\theta = 23^\circ$), we simply count z_S and z_L, the number of contacts in which small and large grains are involved on average as a function of time [Fig. 6(b)]. For the same flow, the position of the center of mass of large grains y_L is reported [Fig. 6(a)]. We see that the segregation process implies a significantly larger coordinance number for large grains. This is somewhat expected since large grains can be surrounded by many small neighbors when the converse is not true. The difference between z_S and z_L is maximum when the mixing is maximum. More significantly, the mean forces f_S and f_L, transmitted by contacts involving at least one small grain and at least one large grain, respectively, reveal a different behavior for the two phases of grains. The normalized mean forces $\hat{f}_S = f_S/m_s g$ and $\hat{f}_L = f_L/m_s g$ (where m_S is the mass of one small grain) are plotted over the course of time in Fig. 6(c). At the start of the flow, the larger grains are at the bottom and are thus submitted to a higher pressure than the smaller grains closer to the surface: the fact that $\hat{f}_S < \hat{f}_L$ is expected. However, as segregation proceeds and larger grains rise to the top, the inequality remains true. This effect becomes more apparent when we normalize the mean forces f_S and f_L by the pressure experienced by the center of mass of each species (y_S and y_L, respectively): $\hat{\hat{f}}_S = f_S/\rho g(H_0 - y_S)$ and $\hat{\hat{f}}_L = f_L/\rho g(H_0 - y_L)$. In doing so, we filter out the influence of the grain position in the flow and stress the fact that forces transmitted by contacts involving large grains are significantly larger than forces transmitted by contacts involving small grains only.

VI. DISCUSSION AND SUMMARY

The aim of this work is to understand the size segregation mechanism in granular chute flows in terms of the pressure distribution within the two phases of grains, large and small, and to relate it to the granular microstructure. Therefore, discrete numerical simulations of bidisperse granular chute flows are systematically analyzed. Based on the theoretical models of Gray and Thornton [33] and Hill and Tan [31], we compute the partial stress tensors associated with the phases of small and large grains while separating the contributions of contact stresses (resulting from forces transmitted at contacts) and kinetic stresses (resulting from grain velocity fluctuations). Comparing the contact pressure in the phases of small grains versus large grains, we observe a slight deviation from a classical mixture, whereby small grains experience less of the gravity gradient than their volume fraction implies. This result supports the possibility of a gravity-driven segregation mechanism as proposed in [33]. We show, however, that the contact stress partition is extremely sensitive to the definition of the partial stress tensors and, more specifically, to the way mixed contacts (namely, contact involving a small grain and a large grain) are handled. As a result, the contact stress partition coefficient is sensitive to the ratio of grain sizes. In that case, the ponderation using grain sizes to split contact forces in the partial stress computation effectively introduces a dependence on the grain size. This dependence may affect the relative values of partial stresses, and introduce a bias in the interpretation of the results. In other words, understanding the role of grains sizes in stress partition becomes uneasy if grains sizes are used at first to define partial stresses.

By contrast, the computation of the partial kinetic stress tensors is more robust since the separation between the large- and small-grain phases, relying on the grains themselves and not on the contacts, is straightforward. Comparing these partial

kinetic stress tensors, we find that the phase of small grains exhibits a significantly higher kinetic pressure than implied by the volume fraction. Computing a kinetic stress partition coefficient in the spirit of [33], we find a value much larger than that obtained for contact stresses and comparable to the values found in [31] and [39]. These results support the existence of a segregation mechanism induced by shear rate gradients as advocated in [31] and [37] and suggest, moreover, that this mechanism might be more important in amplitude than gravity-induced segregation. In our systems, large grains are segregated towards the cooler regions of the flow (the surface) as predicted by kinetic theory [43]. In addition, we evidence an increase in the value of the kinetic stress partition coefficient with the flow shear rate, corresponding to a smaller segregation time, while no such influence on the contact stress partition was observed.

Finally, using a simple approximation for the contact partial stress tensors, we investigate how contact stress partition relates to the flow microstructure. We observe that grain coordinance (namely, a grain's average number of contacts) is greater in the phase of large grains and that contacts involving at least one large grain transmit forces of higher amplitude than other contacts.

Our results do not allow us to decide on either gravity-induced mechanisms or shear-gradient-induced mechanisms as being the most likely. However, the following points should be stressed: (i) the computation of partial contact stress tensors implies a real difficulty due to the existence of mixed contacts; (ii) as a result, the analysis of partial contact stress ratios lacks robustness; and (iii) the analysis of the microstructure might provide a practical proxy for study of gravity-driven segregation.

On the other hand, the robustness of the kinetic stress computation and the sensitivity of the partial kinetic stress partition to the flow state suggest that a parametric study of these quantities varying contact properties, grain sizes, and flow dynamics would lead to interesting new insights into segregation.

ACKNOWLEDGMENTS

This work was supported by the European Union's Seventh Framework Programme (FP7/2007-2013) / Individual European Fellowships PIEF-GA-2011-297843 - GEOGRAF. The authors thank Anthony Thornton for useful comments and suggestions on this work.

[1] J. Bridgewater, W. S. Foo, and D. J. Stephens, Powder Technol. **41**, 147 (1985).
[2] G. Félix and N. Thomas, Earth Planet. Sci. Lett. **221**, 197 (2004).
[3] P. Frey and M. Church, Science **325**, 1509 (2009).
[4] C. G. Johnson, B. P. Kokelaar, R. M. Iverson, M. Logan, R. G. LaHusen, and J. M. N. T. Gray, J. Geophys. Res. **117**, F01032 (2012).
[5] D. M. Powell, Prog. Phys. Geogr. **22**, 1 (1998).
[6] P. J. Rowley, P. Kokelaar, M. Menzies, and D. Waltham, J. Sediment. Res. **81**, 874 (2011).
[7] J. T. Jenkins and S. B. Savage, J. Fluid Mech. **130**, 187 (1993).
[8] J. T. Jenkins and D. K. Yoon, Phys. Rev. Lett. **88**, 194301 (2002).
[9] S. B. Savage and C. K. K. Lun, J. Fluid Mech. **189**, 311 (1988).
[10] G. Berton, R. Delannay, P. Richard, N. Taberlet, and A. Valance, Phys. Rev. E **68**, 051303 (2003).
[11] M. Degaetano, L. Lacaze, and J. C. Phillips, Eur. Phys. J. E **36**, 1 (2013).
[12] V. Garzo and F. V. Reyes, Phys. Rev. E **85**, 021308 (2012).
[13] L. A. Golick and K. E. Daniels, Phys. Rev. E **80**, 042301 (2009).
[14] C. Goujon, B. Dalloz-Dubrujeaud, and N. Thomas, Eur. Phys. J. E **23**, 199 (2007).
[15] F. Guillard, Y. Forterre, and O. Pouliquen, Phys. Rev. Lett. **110**, 138303 (2013).
[16] F. Guillard, Y. Forterre, and O. Pouliquen, Phys. Fluids **26**, 043301 (2014).
[17] L. B. H. May, L. A. Golick, K. C. Phillips, M. Shearer, and K. E. Daniels, Phys. Rev. E **81**, 051301 (2010).
[18] F. Moro, T. Faug, H. Bellot, and F. Ousset, Cold Regions Sci. Technol. **62**, 55 (2010).
[19] J. C. Phillips, A. J. Hogg, R. R. Kerswell, and N. H. Thomas, Earth Planet. Sci. Lett. **246**, 466 (2006).
[20] M. Schröter, S. Ulrich, J. Kreft, J. B. Swift, and H. L. Swinney, Phys. Rev. E **74**, 011307 (2006).
[21] S. Wiederseiner, N. Andreini, G. Épely-Chauvin, G. Moser, M. Monnereau, J. M. N. T. Gray, and C. Ancey, Phys. Fluids **23**, 013301 (2011).
[22] K. van der Vaart, P. Gajjar, G. Epely-Chauvin, N. Andreini, J. M. N. T. Gray, and C. Ancey, Phys. Rev. Lett. **114**, 238001 (2015).
[23] N. Taberlet, W. Losert, and P. Richard, Europhys. Lett. **68**, 522 (2004).
[24] E. Linares-Guerrero, C. Goujon, and R. Zenit, J. Fluid Mech. **593**, 475 (2007).
[25] P. G. Rognon, J.-N. Roux, M. Naaim, and F. Chevoir, Phys. Fluids **19**, 058101 (2007).
[26] B. Yohannes and K. M. Hill, Phys. Rev. E **82**, 061301 (2010).
[27] Yi Fan and K. M. Hill, Phys. Rev. Lett. **106**, 218301 (2011).
[28] A. Tripathi and D. V. Khakhar, Phys. Fluids **23**, 113302 (2011).
[29] B. Marks, P. Rognon, and I. Einav, J. Fluid Mech. **690**, 499 (2012).
[30] A. R. Thornton, T. Weinhart, S. Luding, and O. Bokhove, Int. J. Modern Phys. C **23**, 1240014 (2012).
[31] K. M. Hill and D. S. Tan, J. Fluid Mech. **756**, 54 (2014).
[32] L. Staron and J. C. Phillips, Phys. Fluids **26**, 033302 (2014).
[33] J. M. N. T. Gray and A. R. Thornton, Proc. R. Soc. A **461**, 1447 (2005).
[34] J. M. N. T. Gray and V. A. Chugunov, J. Fluid Mech. **569**, 365 (2006).
[35] J. M. N. T. Gray and B. P. Kokelaar, J. Fluid Mech. **652**, 105 (2010).
[36] C. Meruane, A. Tamburrino, and O. Roche, Phys. Rev. E **86**, 026311 (2012).
[37] Y. Fan and K. M. Hill, New J. Phys. **13**, 095009 (2011).
[38] D. R. Tunuguntla, O. Bokhove, and A. R. Thornton, J. Fluid Mech. **749**, 99 (2014).
[39] T. Weinhart, S. Luding, and A. R. Thornton, AIP Conf. Proc. **1542**, 1202 (2013).

[40] M. Jean and J.-J. Moreau, in *Proceedings of the Contact Mechanics International Symposium*, edited by A. Curnier (Presses Polytechniques et Universitaires Romandes, Lausanne, 1992), pp. 31–48.

[41] J. J. Moreau, Eur. J. Mech. A Solids **13**, 93 (1994).

[42] L. Rothenburg and R. J. Bathurst, Geotechnique **39**, 601 (1989).

[43] M. Larcher and J. T. Jenkins, Phys. Fluids **25**, 113301 (2013).